International Journal of Thin Films Science and Technology

http://dx.doi.org/10.18576/ijtfst/110308

Deposition of Thin Films Materials used in Modern Photovoltaic Cells

Abdelkader BOUAZZA[*]

L2GEGI Laboratory, University of Tiaret, 14000 Tiaret, Algeria

Received: 2 Jun. 2022, Revised: 22 Jul. 2022, Accepted: 2 Aug. 2022
Published online: 1 Sep. 2022.

Abstract: The energy and the angular distribution of atoms are considered two parameters most influential in optimizing the sputtering and subsequently on the deposit, resulting in films having the desired properties (homogeneity in thickness, composition identical to that of the evaporated material). Moreover, a great influence on the shape and quality of thin films is obtained. In this work, a simulation with the Monte Carlo (MC) software SRIM (Stopping and Range of Ions in Matter) is used to calculate the sputtering yield for different energies, and angular distributions of atoms of photovoltaic devices materials (CdS and CIGS) bombarded by different gas particles (Ar, Xe, and Ne). Our results showed that when arriving at a certain energy value E_{max}, the sputtering yield will be in maximum Y_{1max}. Applying this E_{max} and variation in the angular distribution, we will obtain θ_{max} corresponding to the maximum sputtering yield Y_{2max}. These two values (E_{max}, θ_{max}) give the maximum of atoms sputtered, and as a result, the films will be uniform. The obtained results are in very high agreement with other works, which validates our calculations.

Keywords: Thin films, sputtering, Monte Carlo (MC) simulation, CdS, CIS, CIGS.

1 Introduction

With the development of smaller technologies, semiconductor layer depositions are used in several demanding applications such as photovoltaic devices, integrated circuits, transistors, diodes, and RF appliances used in very high-speed devices, and metal layer depositions are used in the manufacture of different kinds of transportation, jewelry, and contacts and also in construction, household items and consumer electronics [1-4].

CdS (Cu_2S) and CIGS ($Cu(In, Ga)Se_2$) are the most important semiconductor materials that can be used to make low-cost photovoltaic devices [5,6]. Therefore, increasing the efficiency of thin-film solar cells is a major research topic today.

High-efficiency CIGS solar cells have been fabricated using the so-called three-stage process [5-7]. This processing method consists of evaporating Cu, In, Ga, and Se pure elements through a three-stage process using four sources. Preparation of the CIGS films with the predetermined composition needs a good and tight control during the deposition process. However, it is hard to manage the metal evaporation sources in the sequence required by the three-stage process when co-evaporating.

Another leading method to fabricate the CIGS absorber layers is via a two-step process, in which the selenization step follows the fabrication step of the metallic precursors [8-13]. The Cu-In-Ga metallic precursor layers are typically prepared by sputtering from multi-sputtering sources.

The thin-film deposition is a technique that allows a thin film or thin layer of material to be deposited on a substrate or previously deposited layers. The term "Thin" is relative, but most depositing techniques make it possible to achieve film thickness of a few nanometers [7,8]

More industrial applications are based on this technology, which is very useful for creating compounds that cannot be manufactured by mass chemistry (processes traditional, such as foundry). In particular, optical manufacturing (for example, reflective or anti-reflective coatings), electronics (insulating, semiconductors, and conductors of integrated circuits), packaging (PET sheets coated with aluminum), and contemporary art [9-11].

The optimization of the deposition parameters leading to films possessing the properties (homogeneity in thickness, composition identical to that of the evaporated material) goes

[*]Corresponding author E-mail: abdelkader.bouazza@univ-tiaret.dz

through many experiments. In order to reduce the duration of this process optimization, it was considered necessary to set up a simulation of the involved in the transport of cash in the presence of a deposit to distributions in thickness and composition of a layer.

The microstructures of these films have been the intention of our group [2-4] to help people in industries by considering diverse parameters influencing the morphology of these films like the distance between the target and substrate, pressure, and the temperature mentioned in this work.

2 Sputtering Technique

Sputtering is a technique used to deposit thin films of a material onto a surface ("substrate"). By first creating a gaseous plasma and then accelerating the ions from this plasma into some source material ("target"), the source material is eroded by the arriving ions via energy transfer. It is ejected in the form of neutral particles - either individual atoms, clusters of atoms, or molecules. As these neutral particles are ejected, they will travel in a straight line unless they contact something - other particles or a nearby surface. If a "substrate" such as a Si wafer is placed in the path of these ejected particles, it will be coated by a thin film of the source material. [12]

- In sputtering, the target material and the substrate are placed in a vacuum chamber.
- A voltage is applied between them so that the target is the cathode and the substrate is attached to the anode.
- A plasma is created by ionizing a sputtering gas (generally a chemically inert, heavy gas like Argon).
- The sputtering gas bombards the target and sputters off the material we would like to deposit.

2.1 Sputtering Process

Over the years, a vast amount of sputter phenomena has been published. Based on analytical models, semi-empirical formulas and computer simulation programs have been developed and published. In the field of theoretical study of sputtering, Thompson's work on energy distribution and Sigmund's for the sputtering yield. After their work, Monte Carlo codes (SIMTRA [13], SRIM [14], etc.) have been developed and have been applied to obtain various properties of sputtering.

As sputter deposition has become popular, problems with it have also been recognized, e.g., the inhomogeneity of the deposition rate on substrate positions. In addition, it has also been understood that the sputtered particles have much larger energies compared to the particles in vacuum evaporation, and affect the properties of deposited films in various ways.

Therefore, it is interesting to know how sputtered particles are transported to the substrate and what energy, flux, and incidence angle they reach therewith38; The Monte Carlo simulation is one of these studies. [1,2]

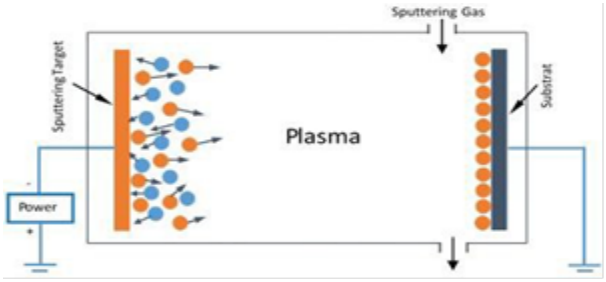

Fig.1: Schematic representation of the sputter deposition process.

In sputter deposition processes (figure1), ions are commonly employed as energetic species because their energy can be easily controlled by using electric fields. An ion source can provide ions, but the most common way is by ionizing inert gas (typically Ar) atoms (i.e., generating a glow discharge/plasma) in an evacuated vessel (referred to as a chamber).

The inert gas ionization occurs by applying a potential difference between the target (serving as a cathode) and an anode. Then positively charged Ar ions are accelerated towards the cathode (negatively biased), providing the energy and momentum necessary for sputtering.

Magnetic fields can be used along with an electric field to confine the plasma close to the target and improve the efficiency of the process. Reactive gases can be added to trigger chemical reactions (primarily on the substrate surface) and thus facilitate the synthesis of multicomponent (compound) films. Sputter deposition is a widely used technique since it combines versatility, control over the composition and microstructure, relatively high deposition rates, and conceptual simplicity. Moreover, it has the advantage of scalability to develop deposition processes and films in a laboratory and transfer them to an industrial environment. [8-11]

2.2 Sputtering Yield Formulas

The sputter yield is the average number of atoms ejected from the target per incident ion. It depends on several variable parameters such as the energy of the ion, the ion incident angle, the masses of the ion and target atoms, the surface binding energy of atoms in the target, and the target's material. [3,4].

$$S = \frac{\text{Number of sputtered atoms}}{\text{Number of incident ions}} \quad (1)$$

S depends on

- type of target atom
- binding energy of target atoms
- relative mass of ions and atoms
- incident ion energy
- angle of incidence of ions

S can range from 0.1 to 10.

2.3 Sputter Yield Formula Obtained by Yamamura

Another approach to calculating the sputter yield is using semi-empirical equations developed by Yamamura. In [15-17]. Yamamura and Tawara [18] extrapolate two formulas, one for heavy ions and another for light ions. In addition to this formula, Yamamura and Ishida [19] have developed a Monte Carlo code that calculates the sputtering yield using the approximation of binary collisions. If we consider an incident particle with atomic mass M1 and atomic number Z1, a target material composed of atoms with atomic mass M2 and atomic number Z2, the sputtering yield for normal incidence Y(E) givenYamamuraetal.is written.

$$Y(E) = 0.042 \frac{Q(Z_2)\alpha^* \left(\frac{M1}{M2}\right)}{U_s} \frac{S_n(\epsilon)}{1 + rK_e\epsilon^{0.3}} \left[1 - \sqrt{\frac{E_{th}}{E}}\right] \quad (2)$$

With energy E in eV, $\in$ is the reduced energy

$$E - \frac{0.03255}{Z_1 Z_2 \left(Z_1^{\frac{2}{3}} + Z_2^{\frac{2}{3}}\right)} \times \frac{M_2}{M_1 + M_2} E, \quad (3)$$

Sn (ϵ) and $k_e\epsilon^{0.3}$ represent, respectively, the electronic and nuclear stopping powers, U_s is the sublimation.

$$r = \frac{W(Z_2)}{1 + \left(\frac{M_1}{7}\right)_3} \quad (4)$$

and α^* depends on the masses report $\frac{\text{M1}}{\text{M2}}$ and represents the collisional inelastic phenomena. It has been tabulated for a large number of ions/target pairs allowing Yamamura obtain a formula for this coefficient:

$$\alpha^* = 0.249 \times \left(\frac{M_2}{M_1}\right)^{0.56} + 0.0035 \times \left(\frac{M_2}{M_1}\right)^{1.5} \text{ when } M_1 \geq M_2 \quad (5)$$

And

$$a^* = 0.0875 \times \left(\frac{M_2}{M_1}\right)^{-0.15} + 0.165 \times \left(\frac{M_2}{M_1}\right) \text{ when } M_1 \leq M_2 \quad (6)$$

Threshold sputtering Eth has also been tabulated from experimental data. Yamamura gave a general expression in which this coefficient depends on the binding energy and mass of ions and target:

$$\frac{E_{tia}}{U_2} = \frac{0.7}{\gamma} \text{ for } M_1 \geq M_2 \quad (7)$$

And

$$\frac{E_{th2}}{U_s} = \frac{1+5.7\times\left(\frac{M_1}{M_2}\right)}{\gamma} \text{ for } M_1 \leq M_2 \quad (8)$$

With

$$\gamma = \frac{4M_1M_2}{(M_1 + M_2)^2} \quad (9)$$

3 Results and discussion

3.1 Monte Carlo Method and Simulation

In general terms, the Monte Carlo method (or Monte Carlo simulation) can describe any technique that approximates solutions to quantitative problems through statistical sampling. However, as used here, 'Monte Carlo simulation' is more specifically used to describe a method for propagating (translating) uncertainties in model inputs into uncertainties in model outputs (results).

The Monte Carlo simulation is a tool to investigate the transport of sputtered atoms and assist engineers in optimizing a given deposition setup. The model is based on numerical Monte Carlo simulations, which are statistical methods that allow one to link a physical value to a random number. Every test is calculated independently of all the others. The final results are the average of the simulations. The Monte Carlo method can provide various kinds of information on the properties of sputtered particle flows deposited on the substrate and allows a considerable contribution to understanding details of the sputtered atom transport in low-pressure gas and energy exchanges between sputtered atoms and gas molecules. In addition, the method is very useful for examining the design of entire sputtering systems, which have a complex geometry [1,2].

3.2 SRIM 2013 (TRIM) Simulation

To estimate the energy distribution of sputtered atoms and ions reflected, we used simulation software called SRIM – "Stopping and Range of Ions in Matter" developed by Ziegler and al. We chose this program because it is easily reachable on the web. This software consists of several modules that can calculate the path of the ions in matter. Among these modules, one that has been used is the TRIM module – Transport of Ions in Matter-.

The method of calculation used is based on Monte Carlo code that simulates the transport and interaction of an ion beam to the surface of a target material and determines the sputtering yield. The model has several input parameters (motion energy, lattice binding energy) but more importantly, for the sputtering portion is the binding energy of the target material: other parameters affect less the results. [14].

3.2.1 Variation of Sputtering Yield for Different Compounds

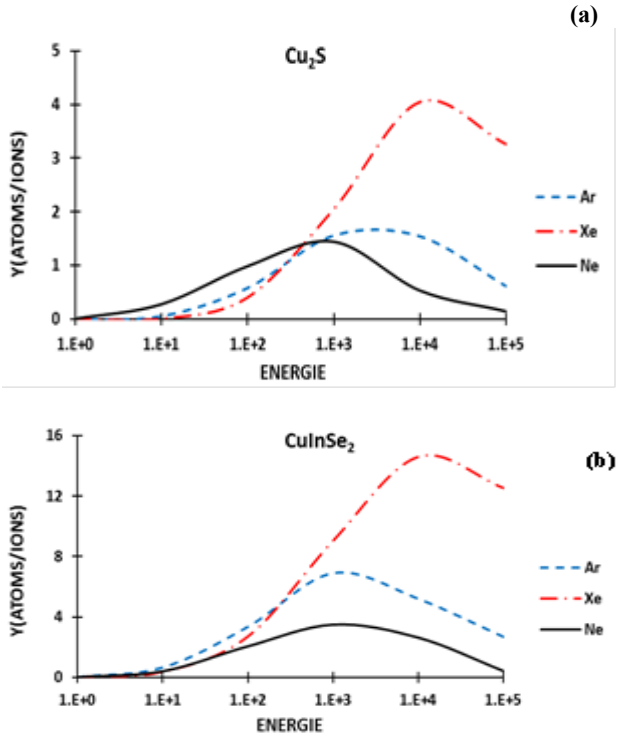

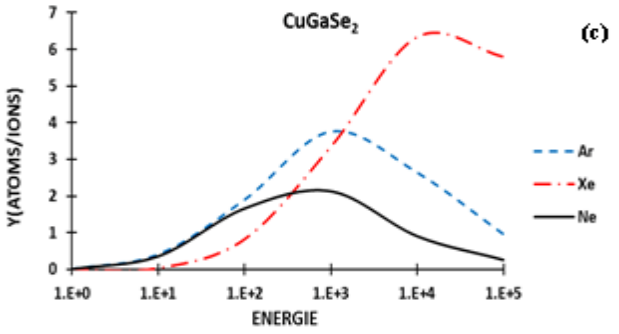

Fig. 2: Sputtering yield as a function of the energy of the bombardment ions (Xe, Ar and Ne) in normal incidence calculated by SRIM for Cu_2S (a), $CuInSe_2$ (b) and $CuGaSe_2$ (c).

3.2.2 Variation of the Ions Sputtering Yield for Different Gas

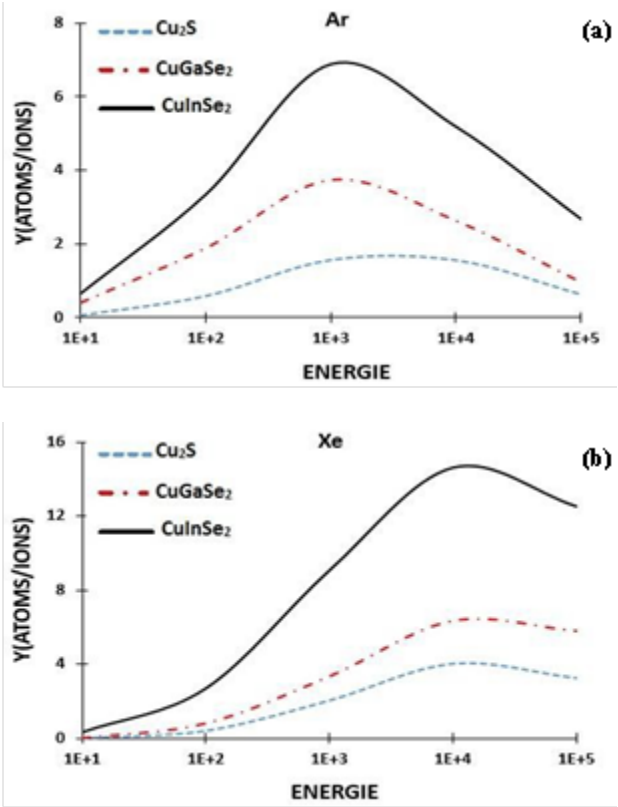

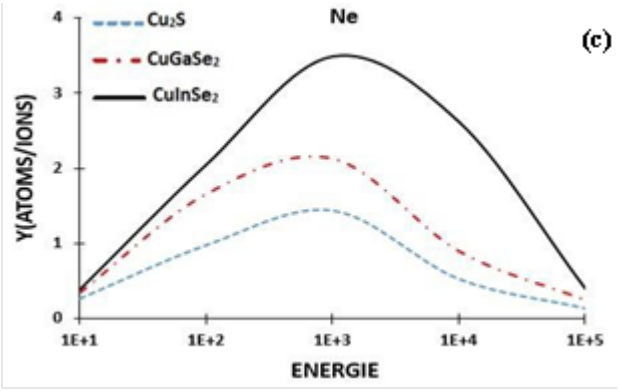

Fig. 3: Sputtering yield for Cu2S, CuInSe2 and CuGaSe2 in normal incidence (θ =0) calculated by SRIM as a function of the energy of the bombardment ions: Ar (a), Xe (b) and Ne (c).

The study of sputter yields has been imposed by the need to control the amount of material deposited. The figures above present the results of the sputter yield calculations obtained by SRIM simulation for different materials as a function of impact energy at normal incidence θ = 0. The simulation of 105 impacts determined each sputter's yield.

Figures 2 and 3 obtain the results by Monte Carlo simulation (SRIM). The chosen targets are photovoltaic solar cells (CdS (Cu2S) and CIGS (Cu(In, Ga)Se2); they are subjected to the bombardment of Xenon (Xe), Argon (Ar), and Neon (Ne) particles, respectively. From these results, it can be seen that the sputtering efficiency of Xenon ions (Xe) is quite high compared to that of Argon (Ar) and Neon (Ne) ions. The particles are ejected if they have enough energy to exceed those of the binding of the target.

At first sight, it is logical to think that if the energy of the incident particle increases, then the number of particles sputtered will grow.

Five areas are distinguished in all the above figures, which represent the variations of the sputter yield Y as a function of energy:

— Zone 1: The energy is too low for the sputtering to occur. There is no actual sputtering threshold. The threshold energy corresponds more to a "cut-off value" introduced to simplify calculations or to a limit below which the measuring devices can no longer detect pulverized particles.

— Zone 2: The sputtering becomes possible. The incident particles have enough energy so that the atoms can break the bonds that bind them to the surface. The coefficient increases rapidly for a small change in energy.

— Zone 3: The coefficient increases linearly with the energy of the incident particles. These coefficient values are high enough to make deposits.

— Zone 4: Incident particles penetrate deeper into the target as their energy increases, and the recoil atoms will be created in larger amounts. The sputtering coefficient is greater than one, which gives more particles ejected than incident particles.

— The sputtering yield (Y) passes through a maximum in Zone 5. The depth of penetration of the incident particles is sufficiently great to cause a decrease in the sputtering yield. The incident particles penetrate so deeply into the target that the recoil atoms cannot escape.

In conclusion, we can decompose the curves of the sputtering yield depending on the energy of the incident particle in three main parts. First, in the threshold sputtering region, no particle has sufficient energy so that the target particles can be ejected. Then the coefficient increases with the energy of the incident particle. Finally, the coefficient passes through a maximum due to a greater penetration depth.

3.3 Influence of the Angle of Incidence

When sputtering material at oblique incidence, a momentum component of the incident ion is parallel to the surface, and some of its energy can be transferred to the surface atoms [20]. As a result, many atoms are then sputtered (Figure 4).

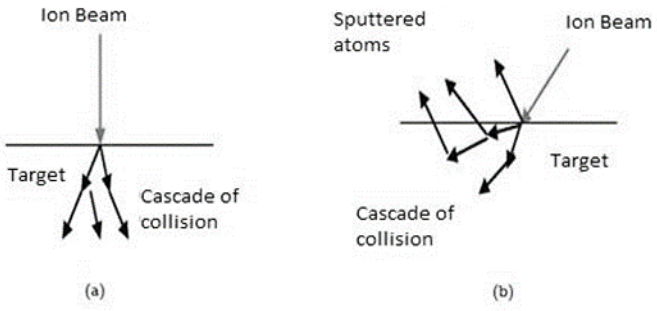

Fig.4: Diagram of the collisional cascade as a function of the incidence angle (a) normal incidence; (b) oblique incidence.

All sputtering yield formulas discussed in previous works (see [3-5]) are valid at normal incidence. However, in 1984, Yamamura [21,22] indicated that in order to take into account the inclination θ of the incident ions, it was enough to multiply the normal incidence of the sputtering yield Y by the following coefficient:

$$\left[(\cos\,\alpha)^{-t}\exp\left(f\left(1-\frac{1}{\cos\,\alpha}\right)\cos\propto_{opt}\right)\right] \qquad (10)$$

Where:

$$f = \sqrt{U_s}\left(0{,}94 - 1{,}33 \times 10^{-3}\frac{M_2}{M_1}\right)$$

$$\propto_{opt} = \frac{\pi}{2} - \frac{a_L U_s}{\gamma E}\left(\frac{1}{2\varepsilon N^{\frac{2}{3}}}\right)^{\frac{1}{2}} \quad (11)$$

$$a_L = 0{,}4685\left(Z_s^{\frac{2}{3}} + Z_g^{\frac{2}{3}}\right)^{-\frac{1}{2}}$$

where γ is the maximum energy transfer coefficient, aL is the Lindhard screening length and N is the target atomic density

3.3.1 Variation of the sputtering yield according to the angles of incidence

In Figure 5, the sputtering yield coefficient reaches a maximum for incidence angles between 60° and 75°, the angle zero corresponding to the normal. The increase in the sputtering coefficient for angles away from the normal incidence results from the increase in the probability of the collisional cascade propagating towards the surface of the cathode.

If the angle of incidence exceeds 80°, then the ions will be reflected without penetration and transfer of momentum to the target.

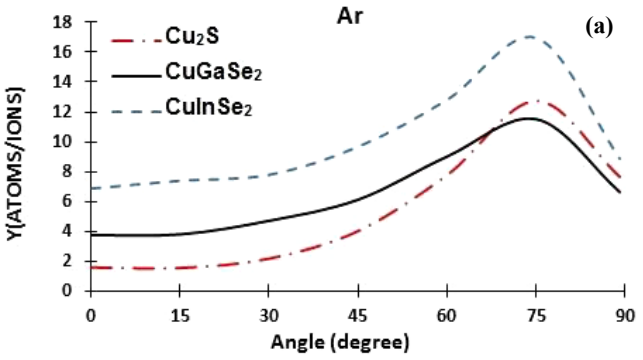

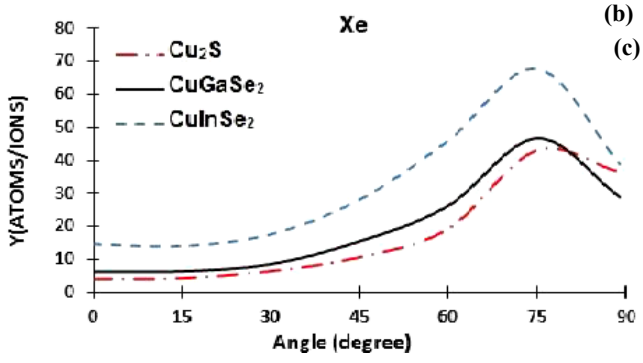

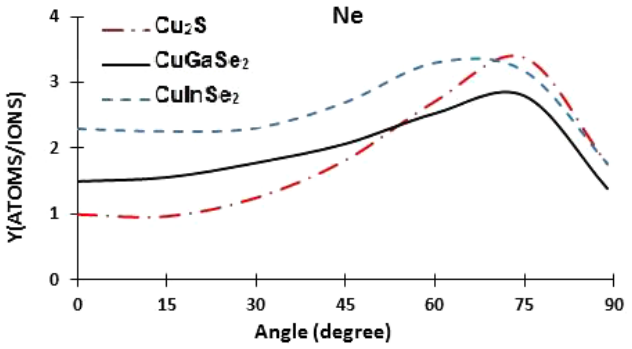

Fig. 5: Sputtering yield as a function of the energy of the bombardment ions (Ar, Xe and Ne) in normal incidence θ = 0 calculated by SRIM for: Cu2S (a), CuGaSe2 (b) and CuInSe2 (c).

The number of particles sputtered will decrease, and therefore the sputtering yield. Once again, this coefficient increases with the mass of the incident ion. We will assume that both ions and fast neutrals arrive with normal incidence on the cathode to alleviate the computation time. This hypothesis is justified by the angular distributions of the incident particles.

3.3.2 Variation in Sputtering Yield According to the Incidence Angles for a fixed Energy

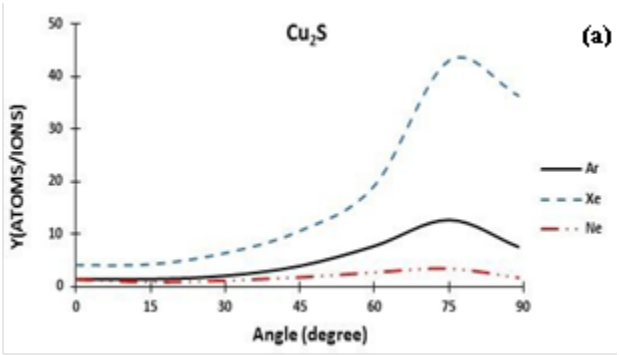

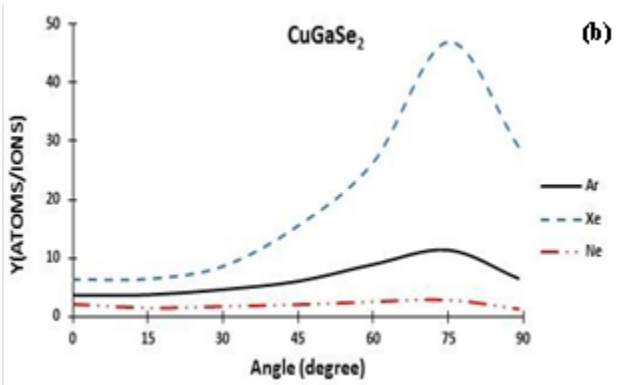

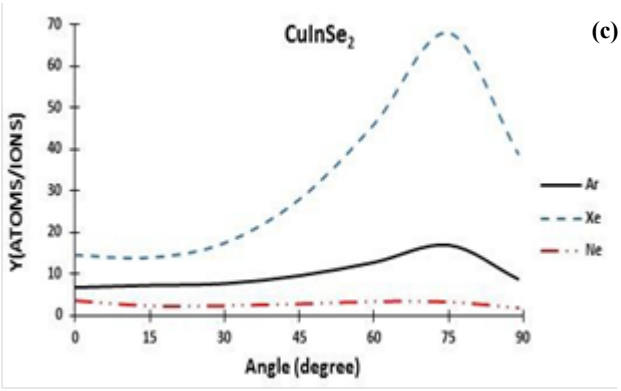

Fig. 6: Sputtering yield as a function of incidence angles for photovoltaic cells Cu2S (a), CuGaSe2 (b) and CuInSe2 (c).

The relationship between the sputtering yield and ion energy for each incidence angle is shown in Figure 6. Sputtering yield graphs are often presented in semi-log format by reason that the value of the yield can vary enormously depending on the energy. For example, the graphs of sputtering yield relative to the incidence angles of the icons shown in Figure 6 indicate that the maximum yield is reached for about an incidence of 75°.

The curves generally show the same form; the yield decreases with the drops of the ion's energy. It is noted that the sputtering yield for ions with 15° of incidence is lower than those for normal incidence (0°), and also, at 30° of incidence, yields are approximately equal to those for normal incidences. All results can be included in a table (Table 1) which indicates the maximum energies and incidence angles for all materials (metals or semiconductors) subjected to ion beam bombardment by different gases (Ar, Xe, and Ne); Emax and θmax obtained and shown in Table 1 give Ymax, and by the way, a maximum of ion sputtered. After that, these ions contribute efficiently to the realization of thin films with an excellent morphology.

Table 1: Maximum energy and incidence angles obtained by SRIM simulation.

		Cu2S	CuGaSe2	CuInSe2
Ar	Emax (KeV)	1	1	1
	θmax (degree)	75	75	75
Xe	Emax (KeV)	10	10	10
	θmax (degree)	75	75	75
Ne	Emax (KeV)	1	1	1
	θmax (degree)	75	75	60

4 Conclusions

With the development of miniature technologies and photovoltaic devices, layers deposition is used in several high demand applications, such as integrated circuits, transistors, diodes, and RF devices used in very high-speed devices, manufacture of different types of transportation, jewelry, eyewear (contacts) as well as in the field of construction, household appliances, and consumer electronics. The microstructures of these films are the object of our interest to serve in the industry of the photovoltaic field, taking into account the various parameters that influence the morphology of these films, such as the energies and incidence angles that become the object of our study, other parameters exhibit in our previous works (see [1-5]) and also in future.

Our work studied and investigated thin films deposition by sputtering CdS and CIGS photovoltaic cells (Cu2S, CuInSe2, and CuGaSe2). The simulations with the Monte Carlo method (SRIM) were used to calculate the sputtering yield *Y* according to the nature of the gases and materials used, and the energies and incidence angles applied, very important parameters in optimizing the yield of deposited thin film layers. The results obtained show that:

- Xenon (Xe) gives very high yields compared to Argon (Ar) and Neon (Ne); it makes sense when knowing that this gas is very inert, easy, and quick to excite. On the other hand, research shows that Ar is the most widely used in terms of its cost and availability despite its advantages.
- In the case of metals, the sputtering yield of CuGaSe2 gives good yields compared to Cu2S and CuInSe2, being closely related to the number of atoms in the outer layer and their bond.
- The maximum sputtering yield (*Y*max) for energies (*E*max) was achieved at around 100 Kev for Xe, 10 Kev for Ar, and 1 Kev for Ne. The incidence angle (θmax) is around 60° to 75°. These factors (*E*max and θmax) correspond to the maximum number of particles sputtered.

We will take these results into account for future works as very important factors that contribute to the development of compounds and devices made in industries by the sputtering method.

References

[1] A. Bouazza, Sputtering of semiconductors, conductors, and dielectrics for the realization of electronics components thin-films. *International Journal of Thin Film Science and Technology, 11(2), pp. 225–232 Carlo Methods Appl, DOI*:10.18576/ijtfst/110210 (2022).

[2] A. Bouazza and A. Settaouti, understanding the contribution of energy and angular distribution in the

morphology of thin films using Monte Carlo simulation. *Monte Carlo Methods Appl, DOI*:10.1515/mcma-2018 (2018).

[3] A. Bouazza, and A. Settaouti, Monte Carlo simulation of the influence of pressure and target-substrate distance on the sputtering process for metal and semiconductor layers. *Mod. Phys. Lett. B, DOI:10.1142/S0217984916502535* (2016).

[4] A. Bouazza and A. Settaouti, Study and simulation of the sputtering process of material layers in plasma. *Monte Carlo Methods Appl, DOI:10.1515/mcma-2016-0106* (2016).

[5] S.E.C. Refas, A. Bouazza, and Y. Belhadji, 3D sputtering simulations of the CZTS, Si and CIGS thin films using Monte-Carlo method, *Monte Carlo Methods and Applications*, DOI: 10.1515/mcma-2021-2094, (2021).

[6] D. Colombara, K. Conley, M. Malitckaya, H.P. Komsa and M.J. Puska, The fox and the hound: in-depth and in-grain Na doping and Ga grading in Cu(In,Ga)Se2 solar cells, *Journal of Materials Chemistry A*, DOI: 10.1039/d0ta01103g (2020).

[7] W. LI, L. YAO, K. LI, et al., Enabling low-temperature deposition of high-efficiency CIGS solar cells with a modified three-stage co-evaporation process. *ACS Appl. Energy Mater.*, DOI: 10.1021/acsaem.9b02025 (2020).

[8] J. Bohdansky, A universal relation for the sputtering yield of monatomic solids at normal ion incidence, *Nuclear Instruments and Methods in Physics Research Section B: Beam Interactions with Materials and Atoms,* DOI:10.1016/0168-583X(84)90271-4 (1984).

[9] M. Castro and C. Tavares, Dependence of Ga-doped ZnO thin film properties on different sputtering process parameters: Substrate temperature, sputtering pressure and bias voltage, *Thin Solid Films,* DOI: 10.1016/j.tsf.2015.04.036 (2015).

[10] D. Depla and W. P. Leroy, Magnetron sputter deposition as visualized by Monte Carlo modeling, *Thin Solid Films,* DOI: 10.1016/j.tsf.2012.06.032 (2012).

[11] U. Dibbern, A substrate for thin-film gas sensors in microelectronic technology, *Sensors Actuators B Chem.2,* DOI:10.1016/0925-4005(90)80010-W (1990).

[12] R. I. Hegde, Film and device characteristics of sputter- deposited hafnium zirconate gate dielectric, *J. Electrochem. Soc*., DOI: 10.1149/1.2890855 (2008).

[13] Ghent University, SIMTRA: SImulation of Metal Transport (2015), http://www.draft.ugent.be.

[14] J. F. Ziegler, SRIM: Stopping and range of ions in matter, preprint (2015), http://www.srim.org.

[15] Martins Saraiva, Marta. *Sputter deposition of MgO thin films: the effect of cation substitution*. Diss. Ghent University (2012).

[16] A. Settaouti and L. Settaouti, Simulation of the transport of sputtered atoms and effects of processing conditions, *Appl. Surface Sci.,* DOI:10.1016/j.apsusc.2008.03.042 (2008).

[17] P. Sigmund, sputtering by ion bombardment theoretical concepts, *Sputtering by particle bombardment I*, DOI: 10.1007/3540105212_7 (1981).

[18] Y. Yamamura, and M. Ishida, Monte Carlo simulation of the thermalization of sputtered atoms and reflected atoms in the magnetron sputtering discharge, Journal *of Vacuum Science & Technology A: Vacuum, Surfaces, and Films, DOI: 10.1116/1.579874* (1995).

[19] Y. Yamamura and H. Tawara, Energy dependence of ion-induced sputtering yields from monatomic solids at normal incidence. *Atomic data and nuclear data tables,* DOI: 10.1006/adnd.1996.0005 (1996).

.[20] D. Piscitelli, Simulation de la pulvérisation cathodique dans les écrans à plasma, *PhD thesis, Université Paul Sabatier, Toulouse* (2002).
10.1006/adnd.1996.0005 (1996).

[21] J.F. Ziegler, Stopping of energetic light ions in elemental matter, *J. Appl. Phys*. DOI: 10.1063/1.369844 (1999).

[22] J.F. Ziegler, SRIM-2003, *Nuclear Instruments and Methods in Physics Research B*, DOI: 10.1016/j.nimb.2004.01.208 (2004)